Research on Biomedical Engineering (2021) 37:193–200
https://doi.org/10.1007/s42600-021-00141-8

ORIGINAL ARTICLE

Comparison of articular and auricular cartilages: decellularization, cell proliferation rate, and infiltration in scaffolds

Liana Hayrapetyan[1] · Hovhannes Arestakesyan[1] · Anush Margaryan[1] · Artem Oganesyan[1] · Vahan Grigoryan[1] · Astghik Karapetyan[1]

Received: 7 September 2020 / Accepted: 29 March 2021 / Published online: 12 April 2021

Abstract

Purpose Various treatment approaches are applied to repair damaged cartilage. However, a developing field of tissue engineering holds a realistic promise to replace injured cartilage tissue using the patient's cells. Using one type of chondrocytes to repair functionally different and far localized cartilage can be feasible from a clinical perspective. Toward this ultimate goal, we aimed to implement key protocols utilized in tissue engineering of articular (AR) and auricular (AU) cartilages.

Methods The experiments were performed according to established protocols that include chondrocyte isolation, assessment of the cell proliferation rates, the degree of cell infiltration in three-dimensional scaffolds, and cartilage decellularization efficacy.

Results The data pointed to significant discrepancies in the size and in vitro chondrocytes proliferation rate isolated from distinct types of cartilage, with AR chondrocytes being 55% larger ($p < 0.01$) while having a slower rate of proliferation. Both collagen- and alginate-based scaffolds showed relevant properties for cell infiltration. Lastly, we have shown that the AR and AU cartilages are decellularized to a different degree ($17 \pm 5.5\%$ vs. $42 \pm 8.5\%$, $p < 0.01$) while using the same SDS-based decellularization protocol.

Conclusion This study will contribute to the global efforts to rebuild damaged cartilage with the help of tissue engineering.

Keywords Cell culture · Chondrocytes · Decellularization · Elastic and hyaline cartilage · Scaffolds · Tissue engineering

Introduction

Cartilage repair is considered to be one of the most challenging clinical problems in orthopedic surgery (Makris et al. 2015). There are two main categories of cartilage damage in the joints: focal and degenerative lesions. The first one is often caused by trauma, osteochondritis dissecans, or osteonecrosis. The second category includes degenerative lesions, which are a result of ligament instability, meniscal injuries, or osteoarthritis (Falah et al. 2010). Current treatment approaches for cartilage lesions include mainly surgical procedures. The latter involves a range of restorative and reparative techniques including arthroscopic debridement, subchondral bone drilling, and perichondral and periosteal arthroplasty. As of today, none of these approaches have provided adequate solutions, as these techniques have shown to be effective only for small focal or medium-sized osteochondral defects (Gugjoo et al. 2016).

Cartilage tissue engineering is a fast-growing scientific field, which aims to develop alternative methods for repair and reconstruction through biomimetic tissue replacements (Zhang et al. 2009). Such products can be useful for many patients who suffer from osteoarthritis, osteoarthrosis, and various meniscal injuries.

Nowadays, active studies are taking place in different levels of cartilage tissue engineering field: from basic science, which goal is to continue revealing the properties of cells, scaffolds, and potential stimulation ways until translational research, aiming to see the behavior of bioprinted cartilages in vivo. However, to date, no clinical trials with 3D-printed cartilages are widely implemented in modern human research (Francis et al. 2018).

The specific goal of this study was to compare the behavior of chondrocytes isolated from different types of bovine cartilage including those harvested from the metacarpal and carpal joints (as an example of hyaline, articular (AR) cartilage) and

✉ Astghik Karapetyan
KarapetyanAstghik84@gmail.com

[1] Laboratory of Immunology and Tissue Engineering, L.A. Orbeli Institute of Physiology NAS RA, Yerevan, Armenia

pinna/external ear (as an example of elastic, auricular (AU) cartilage). We also aimed to compare various available scaffold materials that can support the growth of isolated chondrocytes.

Methods

Chondrocyte isolation and culture As a source of chondrocytes, three different anatomical regions (metacarpal, carpal joints as an AR cartilage, and pinna as an AU cartilage) of the cow were used (Fig. 1). AR and AU cartilages were harvested from market-age cows (20 months old, male) obtained from the local slaughterhouse, Ararat Province, Armenia. The samples were washed in Dulbecco's phosphate-buffered saline (DPBS; MP Biomedicals) to remove the excess of blood and then kept in ice-cold saline supplemented with 1% penicillin/streptomycin. The procedures were done according to previously published protocols with minor modifications (Sabatini et al. 2004; Isogai et al. 2006). Specifically, to isolate chondrocytes, thin slices of AR cartilage (metacarpal and carpal joints) were scraped off with a scalpel, while elastic cartilage (pinna) was cut into ~5 × 5 mm pieces. For the enzymatic digestion, 0.3% collagenase II (Worthington) was used. The samples were transferred into a 5% CO_2 incubator at 37 °C overnight, after which the activity of collagenase was stopped by diluting (1:2) with Dulbecco's modified Eagle's medium (DMEM; Gibco). The digested tissue was filtered through a 100-μm strainer and centrifuged at 2400 rpm for 10 min. After discarding the supernatant, the pellet was resuspended in 5 ml of complete culture medium composed of DMEM supplemented with 10% (v/v) newborn calf serum (NBCS) (#12023C; Sigma) and antibiotics (100×) (#15240062; Gibco). This step was repeated twice. The isolated chondrocytes were counted and seeded in tissue culture-treated dishes at a density of 1.5×10^5 cells/cm^2. The culture plates were incubated in a 5% CO_2 incubator at 37 °C for 24 h to allow cells to attach before the addition of fresh media. Afterwards, the media was replaced every 72 h while observing cell growth using a phase-contrast microscope. On the 14th day, the samples were stained with Alcian Blue dye (Sigma, #A5268) to verify the availability of chondrocytes based on the presence of glycosaminoglycans (GAGs). All required conditions (fresh solution, pH below 2.5) were kept to assure the correct staining of targeted GAGs and to avoid the staining of any negatively charged and H^+ containing not-targeted substances (PromoCell 2015; Quantitative… Cat. No. BP-004). As a negative control, we also stained primary cultures of rat keratinocytes and hepatocytes according to the adopted protocols (Lichti et al. 2008; Severgnini et al. 2012).

Scaffold preparation To seed the chondrocytes, two different scaffolds were tested: collagen and alginate based. The collagen was extracted from a rat tail as described in a previously published protocol (Rajan et al. 2006). To prepare alginate-based sponges, 1% (w/v) of alginic acid sodium salt (BioChemica, #A3249, 0250) was buffered with 10 mM HEPES adjusted to pH 7.4, followed by the addition of 1.8 M $CaCl_2$ in 5:1 ratio. To construct a collagen-based sponge, 4 mg/ml collagen in 0.2 M solution of $CaCl_2$ was allowed to polymerize in the incubator for 30 min at 37 °C.

Cell seeding Cultured chondrocytes were collected by trypsinization and stained with cell tracker dye (Red CMTPX; Invitrogen, Thermo Fisher Scientific, #C34552) according to the manufacturer's protocol. The presence of a cell tracker dye allows longitudinal tracking of cells within the constructs. The same number of cells (2×10^6 cells/ml) was injected into each type of scaffold using a micropipette. The scaffolds with injected cells were put in a cell culture incubator, followed by media change every 72 h. All cell seeding experiments were done under sterile conditions using a biosafety level II cabinet.

Imaging and statistics Phase-contrast imaging was done with a Carl Zeiss Telaval 31 inverted microscope; the pictures were captured using the AmScope camera (MU500, 5MP).

Fig. 1 AR cartilage: metacarpal (**a**) and carpal (**b**); AU cartilage: pinna (**c**). Source of the tissue: mature, 20-month-old cow

Confocal imaging was done with Leica DMi8, TCS SPE, inverted laser scanning confocal microscope. The H&E staining of the samples was conducted by the "HistoGen" Armenian-German pathology center. The obtained image processing and the appropriate measurements were performed using ImageJ—a Java-based open platform for scientific image analysis. Particle counting was done according to the common steps described in ImageJ software protocols, then mean gray values were compared between the groups. To evaluate the decellularization rate of different cartilage types, the saturation of lacunas with cells was counted and compared. Brightness and contrast tools were used to compare staining intensity for Alcian Blue and H&E dyes. The bars are represented as mean with SEM. IBM SPSS Statistics 23.0 software was used to analyze the obtained data. The charts were created using GraphPad Prism 8.0.1. software package.

Decellularization To attain the decellularization of tissues, freshly excised cartilage samples were treated with physical and chemical methods based on the previously published protocol (Kheir et al. 2011). Thin slices were frozen at −20 °C for about an hour after which ice crystals became visible on the tissue surface. Afterwards, slices were left at room temperature for 1 h to thaw. The next two freezing–thawing cycles were made in the same way, but the samples were put in hypotonic (10 mM Tris (hydroxymethyl) aminomethane (#252859; Sigma)-HCl, pH 8.0) solution. As the last cycle ended, the specimens, while still in hypotonic solution, were transferred into an incubator. The next day, the hypotonic solution was removed and 0.1% (w/v) ionic detergent sodium dodecyl sulfate (SDS; Sigma-Aldrich), 4 mg trypsin inhibitor (Gibco #17025-029), and 0.1% (w/v) EGTA were added, after which the samples were incubated. The next day, samples were rinsed with DPBS and incubated in the DPBS solution overnight. Then the slices were fixed in 10% neutral buffered formalin for 24 h. After each step, the samples were incubated for 24 h at 45 °C.

The experiments were conducted in accordance with "Principles of laboratory animal care" and as carried out in accordance with the European Communities Council Directive of September 22, 2010 (2010/63/EU).

Results

Chondrocyte expansion On the eighth day after isolation, the primary culture of AU chondrocytes reached confluency. In contrast, AR chondrocytes had to be cultured for 10 days to reach the same state of confluency (Fig. 2) with metacarpal cells growing slower. Overall, there was no other difference observed between metacarpal and carpal cells cultured, so all the results related to AR cells are shown as a combined outcome of these two anatomical regions.

We then compared the state of cell proliferation on the seventh day after the first passage. The rate of expansion of AU chondrocytes continued to be higher than in AR chondrocytes. We also noticed significant differences in cells' shape with AR chondrocytes being bigger in size and more spindle shaped as compared to AU chondrocytes. The mean perimeter of AR chondrocytes was 31.24 ± 3.02 and for AU: 20.22 ± 2.39 μm ($p < 0.01$) (Fig. 3). At the same time, we noticed the formation of more cell-to-cell connections between AR chondrocytes cultured on the 8th and 17th days (Fig. 4).

Detection of cartilage extracellular matrix (ECM) Alcian Blue dye was used to prove the presence of functionally active chondrocytes. Two other types of primary cells that are known for producing insignificant amount of GAGs were used as negative controls. These included cultures of rat keratinocytes and hepatocytes. The staining intensity of the studied group was visually much higher than in the control groups. Alcian Blue dye was used to prove the presence of functionally active chondrocytes (Fig. 5).

Decellularization degree The decellularization efficiency of AR and AU samples was also examined. The goal of the experiment was to describe the decellularization capacity of different cartilage types. The cartilages cleared from their own cells can be a potential natural scaffold for future implementation, if successful infiltration with the host cells is achieved. The new cells will produce their own ECM, which will replace or enrich the fundament of the already existing natural scaffold. H&E staining has shown that in all samples of decellularized cartilage cellular component decreased, including lacunae of the superficial, middle, and deep zones. This was particularly evident when one compares the histology of partially decellularized versus untreated samples (Fig. 6).

The best results were observed in the case of AU cartilage, where the decellularization rate was $42 \pm 8.5\%$, while in AR cartilage—$17 \pm 5.5\%$ ($p < 0.01$). We also noticed different hues of H&E-stained cartilage due to known differences in the content of the ECM. Specifically, a high amount of collagen in AR cartilage gives it a darker color, while AU cartilage appears pink due to the presence of mostly elastin fibers, which are not stained with H&E.

The properties of the constructed scaffolds and the infiltration of the cells The two types of tested biological scaffolds suitable for three-dimensional seeding of chondrocytes included collagen and alginate based. They took the shape of a custom-made round mold and were mechanically stable for at least 1 week in cell culture conditions. The alginate-based scaffold had a firmer consistency compared to the collagen-

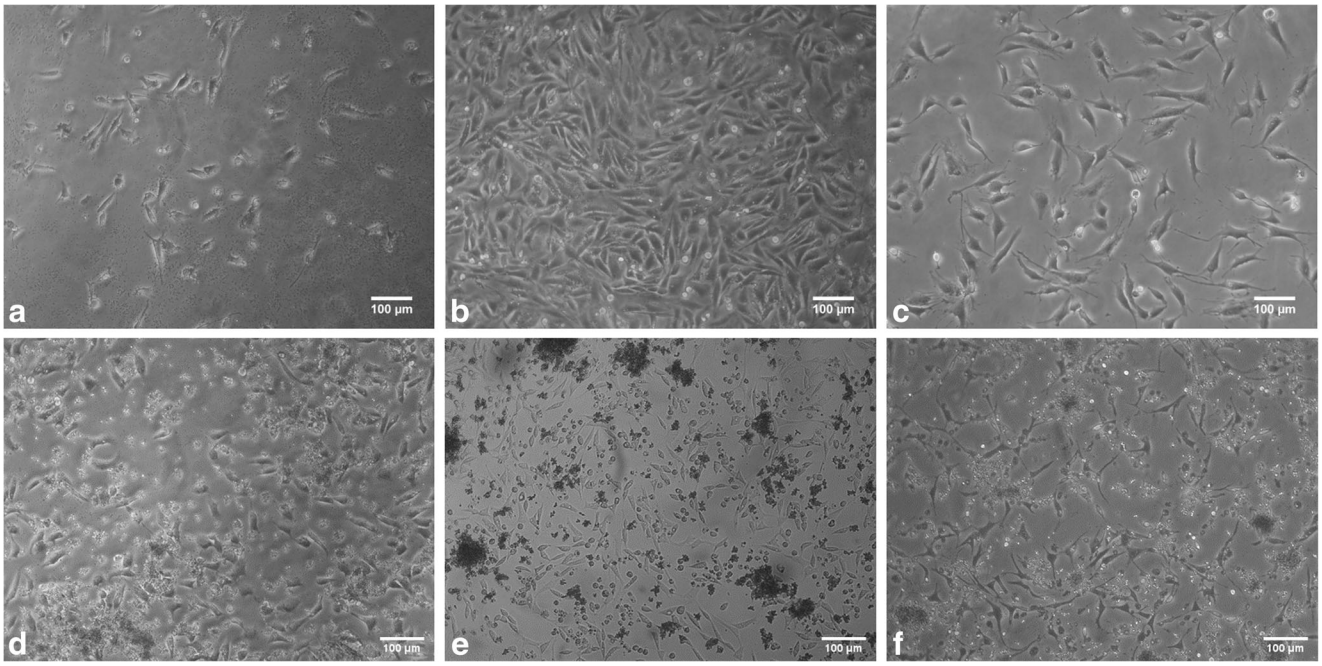

Fig. 2 A gradual change of AR (**a**–**c**) and AU (**cd**–**ef**) chondrocytes. Cell culture on 5th (**a**, **d**), 10th (**b**, **e**), and 14th (**c**, **f**) days. After reaching confluency (**b**), the AR cells were split and cultured into a bigger flask (**c**) where they continue to grow. AU cells were split a few times more during the same period of time because of higher growth rate. Phase-contrast inverted microscope, scale bar = 100 µm

based one, which can be an important factor to consider in surgical handling during implantation. As the infiltrating cells, AR cells were randomly selected for this experiment. 3D imaging of scaffolds using confocal microscopy showed that labeled cells spread into different scaffold layers (Fig. 7).

No significant differences between the 3D distribution of chondrocytes among the two types of tested scaffolds were observed.

Discussion

Cartilage is an important structural component of the body with limited regeneration potential. It consists mostly of ECM proteins and carbohydrates produced by chondrocytes. Depending on the type of ECM, cartilage is categorized into three types: hyaline (e.g., joint surfaces, nasoseptal, costal, tracheal cartilages), elastic (e.g., ear and epiglottis), and fibrocartilage (e.g., intervertebral disk of the spine, ligaments). Cartilage became one of the first targets to be engineered due to its several features: avascular nature, the presence of only one type of cells (chondrocytes), and easy ways to harvest the sample. The abovementioned reasons suggested that ex vivo engineered cartilage can be a promising alternative to repair injured joints and to be used in reconstructive surgery.

AU cartilage belongs to the elastic type of tissue and AR cartilage—to the hyaline. One of the main challenges of cartilage engineering is to characterize the behavior of cells from different cartilage types and to understand if they can be used interchangeably. Evidence for the latter came from an earlier study, which found that AU chondrocytes seeded in 3D scaffold have the potential to be used in the AR cartilage surface reconstruction (Johnson et al. 2004). Thereafter, several studies have attempted to compare chondrocytes isolated from AU

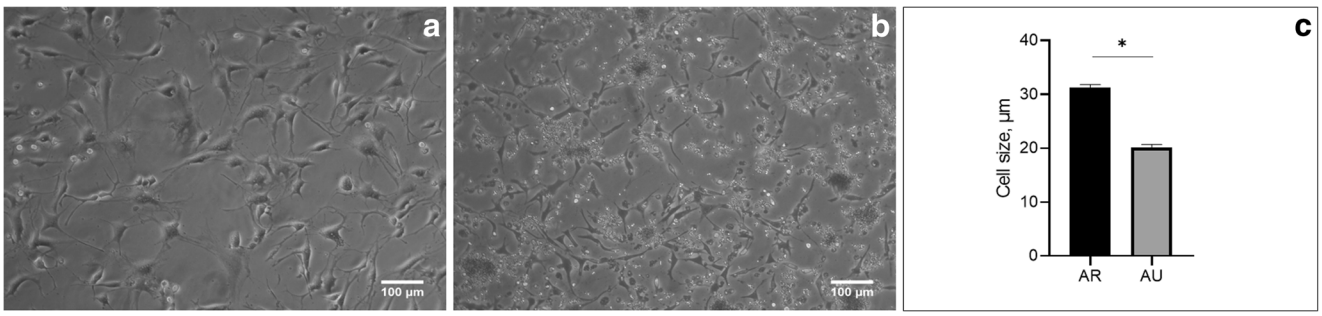

Fig. 3 Cell growth on the 7th day after passage. AR chondrocytes (**a**) are bigger and more spindle shaped than AU (**b**). The graph (**c**) shows the difference in cell sizes in AR and AU cultures ($p < 0.01$). Phase-contrast inverted microscope, scale bar = 100 µm

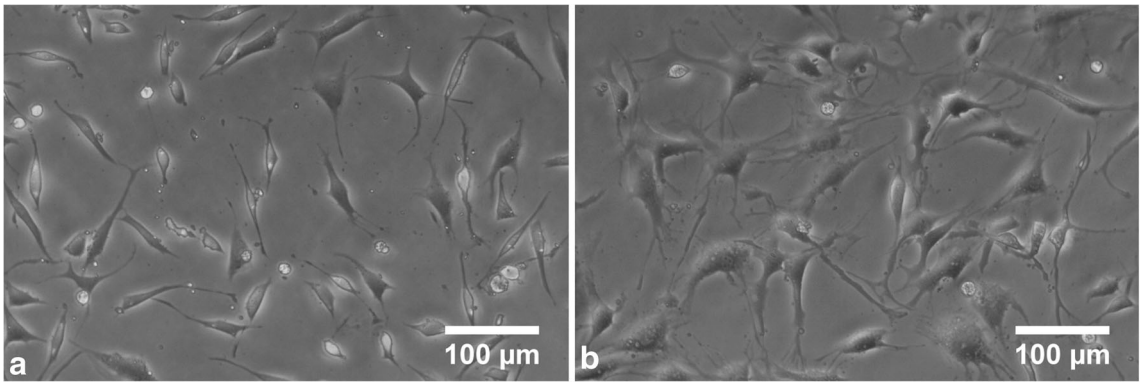

Fig. 4 Illustrative phase-contrast images of cultured AR chondrocytes on 8th (**a**) and 17th (**b**) days showing spindle-shaped cells forming multiple cell-to-cell connections. Phase-contrast inverted microscope, scale bar = 100 μm

and AR cartilages (Isogai et al. 2006; Maličev et al. 2009; Chung et al. 2008). Tay et al., for example, reported that cell yield from human ear cartilage is significantly higher than those from nasal or rib cartilage (Tay et al. 2004). The removal of the cells was significantly easier also in our study, which can be explained by the less firm structure of elastic cartilage that makes up the external ear. At the same time, the researchers within the same study did not find any differences in proliferation rates of isolated chondrocytes from the abovementioned samples. In addition, in the absence of

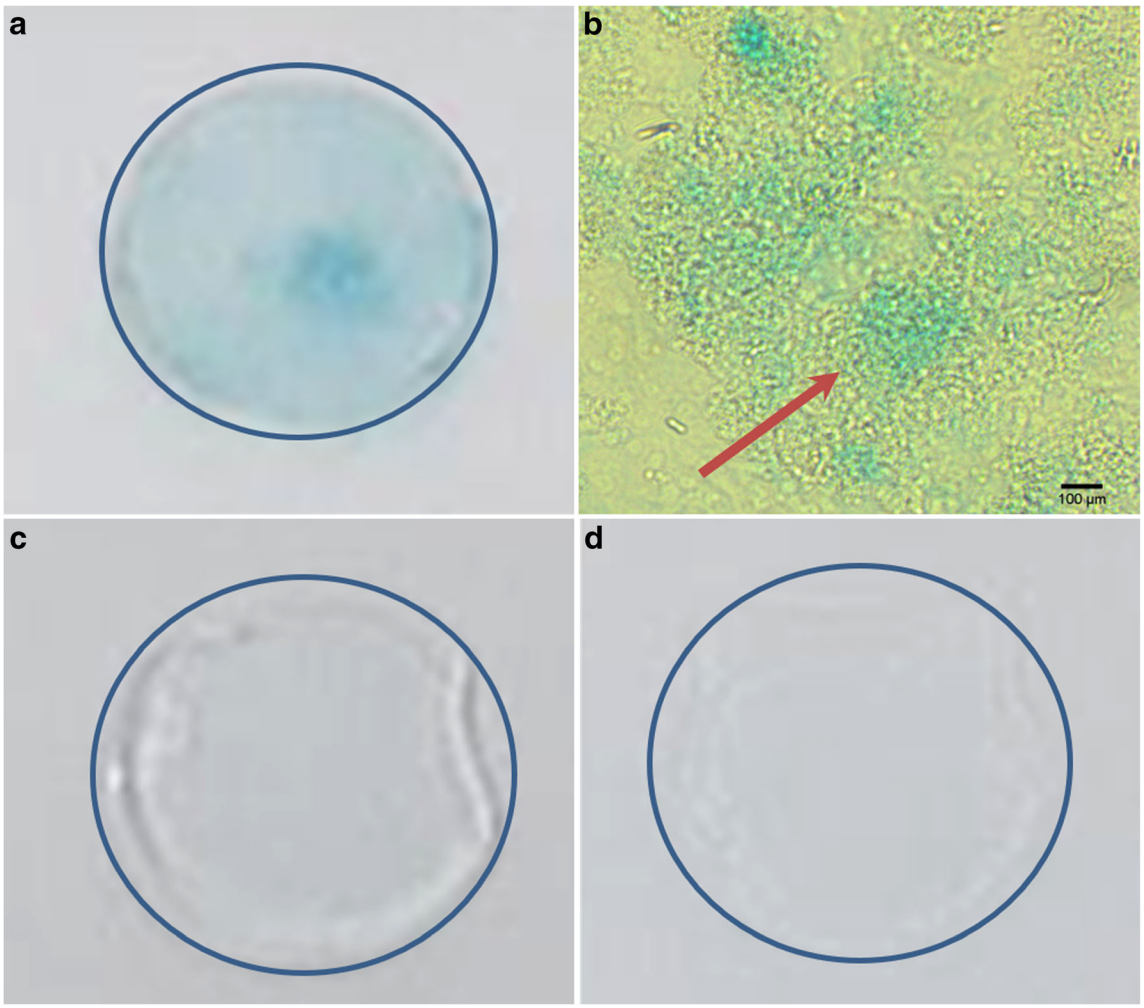

Fig. 5 The staining of chondrocyte cultures for GAGs. Staining: Alcian Blue. Top row (**a**, **b**): positively stained chondrocyte cultures and a close-up showing accumulation of GAGs (arrow). Bottom row: appearance of identically stained rat keratinocytes (**c**) and hepatocytes (**d**). Light microscope, scale bar = 100 μm

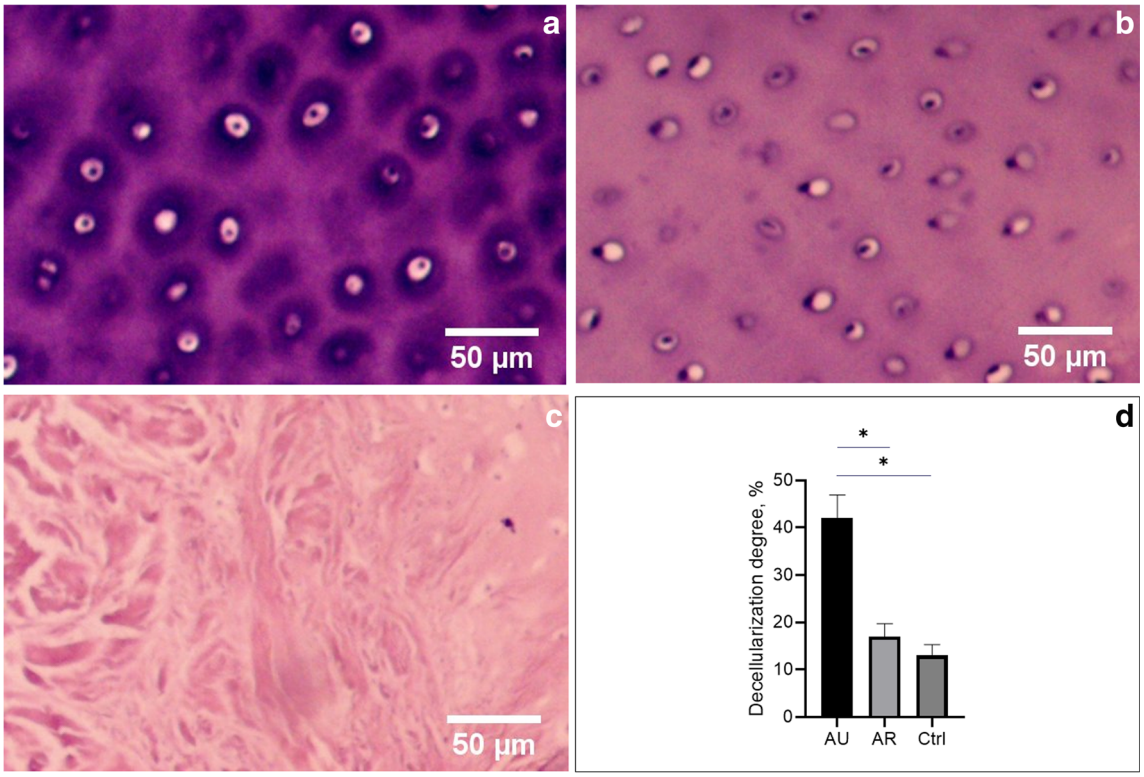

Fig. 6 Staining of the control and decellularized samples with H&E. Comparing with the control group (**a**), AU samples (**c**) lost 42% of cells ($p < 0.01$). Small changes are detected in treated AR (**b**) samples. The percent of lost cells are shown in the graph (**d**). Light microscope, scale bar = 50 µm

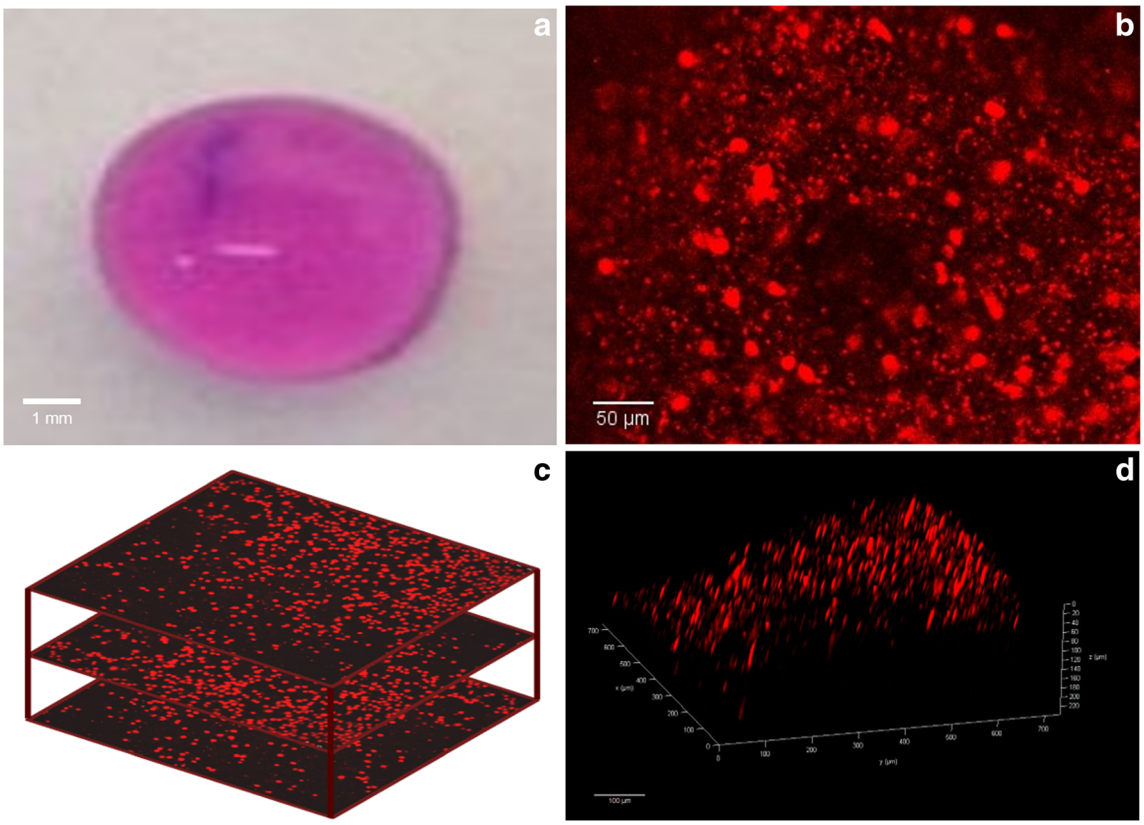

Fig. 7 Cell seeding in the collagen-based 3D scaffold. AR chondrocytes cultured for 17 days are stained with Red CMTPX (**b**), seeded in the collagen-based scaffold (**a**) followed by optical Z-sectioning using confocal microscopy. Schematic illustrations of cell infiltration among the scaffold (**c**) and confocal image of AR chondrocytes in the collagen-based scaffold (**d**) are shown. Confocal microscope

growth factors, both AR and AU chondrocytes showed identical ability to produce new ECM and particularly collagen type II in three-dimensional pellets (Tay et al. 2004). In contrast to this study, Isogai et al. found out that although AU chondrocytes exhibit lesser ability to proliferate compared to AR (costal and nasoseptal) chondrocytes, they are, in fact, can produce greater amounts of ECM (Isogai et al. 2006).

Our data add to this apparent controversy by showing that the proliferation rate of the chondrocytes derived from AU cartilage is higher than in the case of the AR cartilage. Potential reasons why our results were different from the above-cited Tay et al. and Isogai et al. include variations in study objectives and their ages, harvested anatomical regions, the time required from harvesting to isolation, and other non-considered factors.

The second component of engineered tissue is scaffold material. The latter acts as functional support helping the cells to adhere and proliferate. Scaffolds can be made from natural, synthetic materials, or their combination (Grigore 2017). A number of critical issues such as producing structurally firm scaffolds, while providing a proper environment for the cells to form a functionally active tissue, remain an active area of research (O'brien 2011). Safari et al. showed an interesting approach by replacing the classical scaffold options with a human umbilical cord–derived scaffold, which demonstrated the properties similar to the gelatin-based scaffold (Safari et al. 2019). In this work, we successfully adapted protocols to decellularize cartilage tissue by aiming to reveal the future potential of natural closest scaffold type, as well as to seed isolated chondrocytes into the dimensional biological scaffolds made from collagen and alginate.

Conclusion

In conclusion, we succeeded in isolating two types of chondrocytes, culture and seeding them into ECM-based (collagen) and synthetic (alginate) scaffolds. Our data suggest that the proliferation rate of the chondrocytes derived from AU cartilage is significantly higher than in the case of the AR cartilage. We have also shown that different types of cartilage are decellularized to a different degree while subjected to the same protocol. Our studies contribute to future efforts to use decellularized cartilage as a potential scaffold for treating the focal defects as it provides a supportive environment for chondrocyte seeding.

Acknowledgments This work was enabled by the United States Fulbright program via US Scholar award to Dr. Narine Sarvazyan. We gratefully acknowledge Drs. Sarvazyan and Karabekian for their advice and experimental guidance and administration of L.A. Orbeli Institute of Physiology NAS RA for logistical support. We also want to thank "HistoGen" Armenian-German pathology center (Yerevan, Armenia) for providing histological assays.

Code availability Not applicable.

Authors' contributions All authors equally contributed to the experimental and theoretical parts of the study as well as participated in the writing of the manuscript.

Funding Not applicable.

Data availability Not applicable.

Declarations

Conflicts of interest/competing interests The authors declare that they have no conflict of interest.

Ethics approval The experiments were conducted in accordance with "Principles of laboratory animal care" and as carried out in accordance with the European Communities Council Directive of September 22, 2010 (2010/63/EU).

Consent to participate Not applicable.

Consent for publication Not applicable.

References

Chung C, Erickson IE, Mauck RL, Burdick JA. Differential behavior of auricular and articular chondrocytes in hyaluronic acid hydrogels. Tissue Eng Part A. 2008;14:1121–31. https://doi.org/10.1089/ten.tea.2007.0291.

Falah M, Nierenberg G, Soudry M, Hayden M, Volpin G. Treatment of articular cartilage lesions of the knee. Int Orthop. 2010;34:621–30. https://doi.org/10.1007/s00264-010-0959-y.

Francis SL, Di Bella C, Wallace GG, Choong PFM. Cartilage tissue engineering using stem cells and bioprinting technology—barriers to clinical translation. Front Surg. 2018;5. https://doi.org/10.3389/fsurg.2018.00070.

Grigore ME. Biomaterials for cartilage tissue engineering. J Tissue Sci Eng. 2017;08. https://doi.org/10.4172/2157-7552.1000192.

Gugjoo MB, Amarpal, Sharma GT, Aithal HP, Kinjavdekar P. Cartilage tissue engineering: role of mesenchymal stem cells along with growth factors & scaffolds. Indian J Med Res. 2016. https://doi.org/10.4103/0971-5916.198724.

Isogai N, Kusuhara H, Ikada Y, Ohtani H, Jacquet R, Hillyer J, et al. Comparison of different chondrocytes for use in tissue engineering of cartilage model structures. Tissue Eng. 2006;12:691–703. https://doi.org/10.1089/ten.2006.12.691.

Johnson TS, Xu JW, Zaporojan VV, Mesa JM, Weinand C, Randolph MA, et al. Integrative repair of cartilage with articular and nonarticular chondrocytes. Tissue Eng. 2004. https://doi.org/10.1089/ten.2004.10.1308.

Kheir E, Stapleton T, Shaw D, Jin Z, Fisher J, Ingham E. Development and characterization of an acellular porcine cartilage bone matrix for use in tissue engineering. J Biomed Mater Res A. 2011;99A:283–94. https://doi.org/10.1002/jbm.a.33171.

Lichti U, Anders J, Yuspa SH. Isolation and short term culture of primary keratinocytes, hair follicle populations, and dermal cells from newborn mice and keratinocytes from adult mice, for in vitro analysis

and for grafting to immunodeficient mice. Nat Protoc. 2008;3:799–810. https://doi.org/10.1038/nprot.2008.50.

Makris EA, Gomoll AH, Malizos KN, Hu JC, Athanasiou KA. Repair and tissue engineering techniques for articular cartilage. Nat Rev Rheumatol. 2015;11:21–34. https://doi.org/10.1038/nrrheum.2014.157.

Maličev E, Kregar-Velikonja N, Barlič A, Alibegović A, Drobnič M. Comparison of articular and auricular cartilage as a cell source for the autologous chondrocyte implantation. J Orthop Res. 2009;27:943–8. https://doi.org/10.1002/jor.20833.

O'brien FJ. Biomaterials & scaffolds for tissue engineering. Materials today. 2011;14:88–95. https://doi.org/10.1016/S1369-7021(11)70058-X.

PromoCell GmbH. Chondrogenic differentiation and analysis of MSC. 2015. http://www.promocell.com/f/2017/11/Chondrogenic_Differentiation_and_Analysis_of_MSC-1.pdf

Quantitative dye-binding assay for the in vitro analysis of sulfated glycosaminoglycans in synovial fluid, blood and tissue extracts, sGAG Assay, Cat. No. BP-004. https://search.cosmobio.co.jp/cosmo_search_p/search_gate2/docs/KAM_/BP004.20120409.pdf

Rajan N, Habermehl J, Coté MF, Doillon CJ, Mantovani D. Preparation of ready-to-use, storable and reconstituted type I collagen from rat tail tendon for tissue engineering applications. Nat Protoc. 2006;1:2753–8. https://doi.org/10.1038/nprot.2006.430.

Sabatini M, Pastoureau P, De Ceuninck F. Methods in molecular medicine. Cartilage and Osteoarthritis. Volume 1. Cellular and molecular tools: Humana Press; 2004.

Safari F, Fani N, Eglin D, Alini M, Stoddart MJ, Baghaban EM. Human umbilical cord-derived scaffolds for cartilage tissue engineering. J Biomed Mater Res A. 2019. https://doi.org/10.1002/jbm.a.36698.

Severgnini M, Sherman J, Sehgal A, Jayaprakash NK, Aubin J, Wang G, et al. A rapid two-step method for isolation of functional primary mouse hepatocytes: cell characterization and asialoglycoprotein receptor based assay development. Cytotechnology. 2012;64:187–95. https://doi.org/10.1007/s10616-011-9407-0.

Tay AG, Farhadi J, Suetterlin R, Pierer G, Heberer M, Martin I. Cell yield, proliferation, and postexpansion differentiation capacity of human ear, nasal, and rib chondrocytes. Tissue Eng. 2004;10:762–70. https://doi.org/10.1089/1076327041348572.

Zhang L, Hu J, Athanasio KA. The role of tissue engineering in articular cartilage repair and regeneration. Crit Rev Biomed Eng. 2009;37:1–57. https://doi.org/10.1615/critrevbiomedeng.v37.i1-2.10.